

Locating the blazar gamma-ray emitting zone from astrometric VLBI and *Gaia* data?

Sol, H el ene^{a,*}, Lambert, S ebastien^b, and Pierron, Antonin^b

a LUTH, Observatoire de Paris, Universit  PSL, CNRS, Universit  Paris-Cit ,
Place J. Janssen, 92195, Meudon, France

b SYRTE, Observatoire de Paris, Universit  PSL, CNRS, Sorbonne Universit , LNE,
77 avenue Denfert-Rochereau, 75014, Paris, France

E-mail: helene.sol@obspm.fr, sebastien.lambert@obspm.fr

Although current emission models are generally able to account for the observed spectra of blazars from radio to TeV energies, unknowns remain on several fundamental questions such as the nature of the emitting particles, leptons or hadrons, the mechanism dominating the particle acceleration, and the origin of ultrafast variabilities. Some of the degeneracy between models could be removed by better localization of the γ -ray emission zone, which can be constrained but is not directly fixed by the low angular resolution γ -ray data. Different locations can be considered such as the black hole magnetosphere, the radio core, the jet and knots detected in VLBI, or even more distant structures along the jets. Confronting the γ -ray data with the very high precision absolute astrometry in the radio and optical ranges from the permanent geodetic VLBI program and the ESA *Gaia* mission should shed new light on this question.

Here we aim to analyze a sample of 816 active galactic nuclei (AGN) dominated by blazars, including a population of 214 BL Lacs and 488 Flat Spectrum Radio Quasars (FSRQ), cross-identified from the *Gaia* EDR3, the third radio International Celestial Reference Frame (ICRF3), and the *Fermi*-LAT 4FGL catalogs. For a first sample of AGN for which Very Long Baseline Interferometry (VLBI) radio maps are available from the MOJAVE program, and within astrometric errors of less than 0.1 mas, most optical emissions (typically 90 %) detected by *Gaia* appear to be associated either with the VLBI radio core, or with a radio knot downstream in the jet at the parsec scale. We investigate the general trends of the main sample in terms of AGN classification, *Gaia* color indices, and GeV emission, and discuss in particular the observed decrease of γ -ray fluxes with the angular distance of the optical emission zone from the radio centroid, as well as the difference in behavior identified between the two populations of BL Lacs and FSRQ.

7th Heidelberg International Symposium on High-Energy Gamma-Ray Astronomy (*Gamma2022*)
4-8 July 2022
Barcelona, Spain

*Speaker

  Copyright owned by the author(s) under the terms of the Creative Commons Attribution-NonCommercial-NoDerivatives 4.0 International License (CC BY-NC-ND 4.0).

<https://pos.sissa.it/>

1. Introduction

The location of the γ -ray emitting zone(s) in blazars is still a critical open question. Several sites have been proposed such as black hole magnetosphere, base of jet, ‘inside’ or ‘outside’ the broad line region (BLR), VLBI knot, and large scale jet component (see Rieger, this proceedings). Despite this range of possibilities, tensions remain for some sources, for instance when the lack of BLR γ - γ absorption features (see Foffano, this proceedings) suggests a γ -ray emission from ‘outside’ the BLR, which is not easy to reconcile with severe constraints imposed on the size of the emitting VHE zone for fast varying blazars such as 3C 279 or PKS 1222+216. Identifying the true location should better constraint the properties of the VHE zone and could break degeneracies between various scenarios of blazar emission by providing a better view on the properties of the local magnetic field, the nature of emitting particles (leptonic versus hadronic models), the dominant particle acceleration mechanism, and the origin of variability.

A MWL approach is mandatory to explore blazars at very small angular scales, in particular in the radio and optical ranges. Indeed there are growing evidences for correlation between some HE and VHE flares and events seen by radio VLBI in a few sources: radio core flux variations, emergence of new knots at jet base, appearance of stationary features (e.g. [Lico et al, 2022](#)). Beyond the study of individual sources, statistical approaches allow to better identify general trends. For instance, a long term joint VLBI-*Fermi* monitoring of 331 AGN has shown strong correlations between *Fermi*-LAT flux and delayed radio fluxes, from the radio core, and from the radio jet ([Kramarenko et al, 2022](#)). Temporal correlations often observed between optical, X-ray, and γ -ray fluxes also suggest a common emission region and correlated mechanisms (see Otero-Santos, this proceedings).

Astrometric data on AGN from geodetic VLBI and from the *Gaia* satellite offer the possibility of large statistical analyzes. Studies of the VLBI-*Gaia* offsets recently showed that the optical *Gaia* centroid is preferably located in the jet and found the coincidence of some optical centroids with VLBI knots often stationary and with high linear polarization ([Kovalev et al. 2020](#), [Lambert et al. 2021](#)). This suggests that these optical centroids are dominated by non-thermal synchrotron emission. In standard emission models, HE and VHE γ -rays can then be expected from the same region by inverse-Compton emission in the leptonic scenario, or when the optical synchrotron emission is due to secondary particles in the hadronic scenario. In both cases, these optical centroids can indicate location of the γ -ray emitting zone. However, the complexity of the sky in the optical range (see Padovani, this proceedings) makes the situation more difficult because many other optical radiations can influence the *Gaia* centroid position and contaminate the non-thermal optical emission, due to accretion disks and BLR/NLR, stellar halos, gaseous components, host-galaxies, as well as obscuration effects, which requires further analysis.

In this contribution, we consider the sample of AGN cross-identified between the International Celestial Reference Frame (ICRF3) and the *Gaia* Early Data Release (EDR3) which provide absolute sub-mas astrometry at three radio frequencies (ICRF3) and in the optical range (*Gaia*). The ICRF and *Gaia* precisions are comparable and of the order of 0.1 mas. As shown in Fig.1, positional differences reveal some significant offsets between radio and optical centroids at the milli-arcsecond (mas) level, which by itself raises question for the alignment and tying of the reference frames.

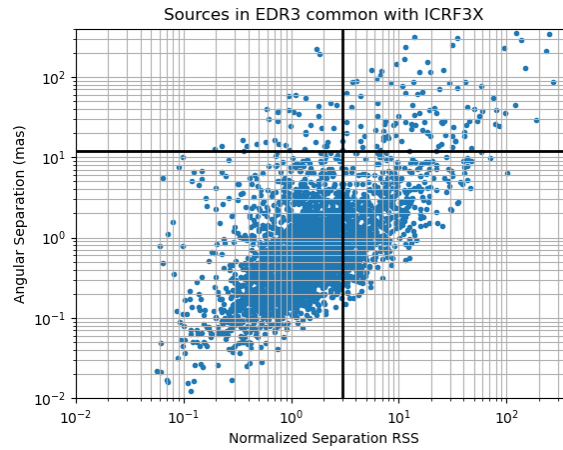


Fig.1 - Offsets between ICRF3 and *Gaia* EDR3 centroids for more than 3500 cross-identified sources

2. Analysis of AGN samples from ICRF3 and *Gaia*

2.1 AGN from ICRF3, *Gaia* and the MOJAVE program

Gathering the ICRF3 positions at ‘X-band’ at 8.4 GHz (*Charlot et al, 2020*), the *Gaia* EDR3 positions (*Brown et al, 2021*), and the MOJAVE modelfits at 15 GHz (*Lister et al, 2021*), we have analyzed a preliminary sample of about 350 AGN and studied the possible coincidence between the *Gaia* centroid and the different MOJAVE core and jet components by looking for the radio structure located closest to the optical centroid.

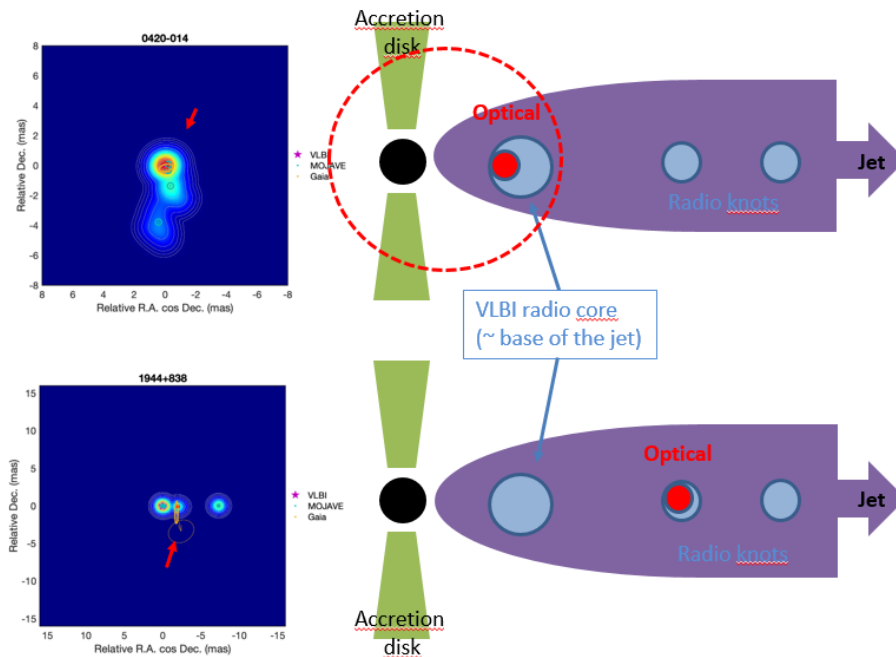


Fig.2 - On the right, sketch for two main populations of VLBI-*Gaia* blazars, whose optical centroid (red) is associated with the disk or with the radio core (upper case), or with a radio knot downstream in the jet (lower case). On the left, VLBI maps of sources representative of the two populations, with MOJAVE components (color scale) and *Gaia* centroid positions (yellow disks, indicated by red arrows).

Only about 11% of the sources showed no apparent coincidence. The majority of the AGN showed significant coincidence either with the VLBI radio core ($\sim 24\%$), or with the radio core and a radio knot at the base of the jet ($\sim 36\%$), or with a radio knot downstream in the VLBI jet ($\sim 28\%$). Apart from the few specific cases without coincidence, we have therefore identified two main populations of AGN illustrated in Fig.2, in which the optical emission appear related either to the central engine, or to the jet.

2.2 AGN from ICRF3, Gaia and the Fermi-LAT catalog

In a second approach, we consider again the centroids of the ICRF3 ‘X-band’ at 8.4 GHz and the optical *Gaia* centroids, together with their EDR3 ‘BP-RP’ color index, and the 1-100 GeV γ -ray fluxes F_γ of the *Fermi*-LAT from the 4FGL-DR3 catalog (Abdollahi et al, 2022), with the classification of the sources given by the *Fermi* catalog. The resulting sample gathers 816 AGN among which 488 confirmed flat spectrum radio quasars (FSRQ) and 214 confirmed BL Lacs. It is therefore dominated by FSRQ unlike the *Fermi* catalog of blazars, which reflects the selection effects by the ICRF3 and the *Gaia* catalogs. We explore the properties of this new sample according to the main parameter of our study, namely the angular distance or separation r between the positions of the radio centroid (‘X-band’ of the ICRF3) and of the optical centroid (*Gaia*). The uncertainty on the separation is computed according to appropriate astrometry formulae (Mignard et al, 2016; Charlot et al, 2020).

Approximately 83% of the entire sample shows negligible or no separation at all ($r/\sigma < 3$) compatible with the coincidence of the two centroids, but 17% exhibits significant separation ($r/\sigma > 3$). The ratio is significantly different when considering only the FSRQ (resp. BL Lacs), with 88% (resp. 76%) of coincidences, and 12% (resp. 26%) of significant non-zero separations.

As shown in Fig. 3, the F_γ globally decreases with increasing separation r , although a plateau appears with a secondary peak at separation $r_p \sim 0.5$ to 0.6 mas for the population of BL Lacs. FSRQ appear overall bluer than BL Lacs, which could be due to the contribution of bright optical-UV disks (absent in BL Lacs) to their optical emission. If we identify the radio centroids with the radio cores, as often assumed for core-dominated sources, such disk effect could also explain why FSRQ appear bluer at small r , but a priori not the increase of their F_γ with reddening. There are some hints of the existence of two subgroups of BL Lacs, namely a subgroup 1 with small to moderate separation ($r \leq r_p$), globally higher F_γ , and intermediate BP-RP color index, and a subgroup 2 with larger separation ($r \geq r_p$), globally weaker F_γ , and redder color index.

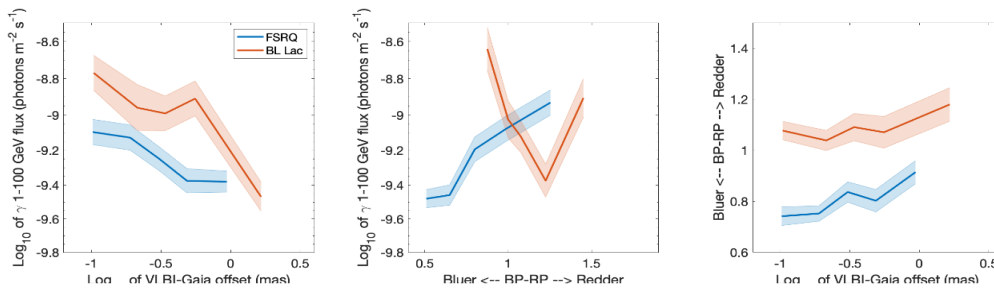


Fig.3 - Distribution of the FSRQ and BL Lac populations in the plans $\log F_\gamma - \log r$ (left), $\log F_\gamma - \text{BP-RP}$ (middle), and $\text{BP-RP} - \log r$ (right). Here the median of y-quantity is given with its uncertainty in bins of x-quantity with equal number of sources.

To further investigate the trends in the parameter space r , F_γ and BP-RP, we present in Fig.3 and 4 the Kernel Smoothing Density (KSD) of the distribution patterns for different sub-samples.

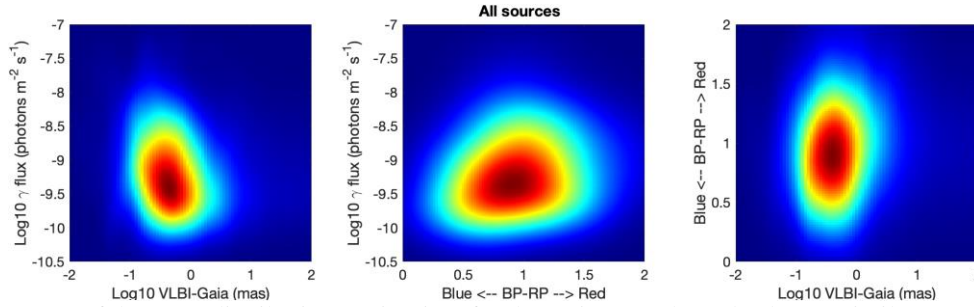


Fig.4 - KSD of the same distributions as in Fig.3 for the entire sample. Indeed, very similar patterns are obtained for the sub-sample of sources with small separation ($r/\sigma < 3$), and only slightly modified patterns for the sub-sample of FSRQ (not shown here).

The KSD approach confirms that the F_γ globally decrease and the optical centroids become redder as r increases for (1) the entire sample, for (2) the sources with small r , and to some extent for (3) the FSRQ which dominate the sample (see Fig.4). Conversely, the F_γ increase overall with redder color indices. The highest F_γ are found for small r and intermediate color indices, and the brightest γ -ray sources globally correspond to optical emission close to the core and base of the jet if we again identify the radio centroid with the radio core. At such small r and neglecting host-galaxy contamination, the optical emission is most likely dominated by a bright disk or by the non-thermal core, depending on the intensity and frequency of the synchrotron peak. As FSRQ dominate the sample, bright disks (with harder optical spectra than synchrotron jet) can induce bluer optical centroids on the average at small r . However, this disk effect does not seem to explain why the F_γ globally increase with decreasing r and with redder color index. Indeed in this sample the presence of bright disks seems to be associated with lower F_γ as BL Lacs show higher F_γ than FSRQ. This could be due to a selection effect by *Gaia* which has a limiting magnitude of 21 and provides an optical flux-limited sample. On the average, the numerous faint *Gaia* sources with brighter disk show weaker optical non-thermal emission (and reciprocally), inducing a trend in favor of smaller F_γ in the presence of bright disk and of bluer color index.

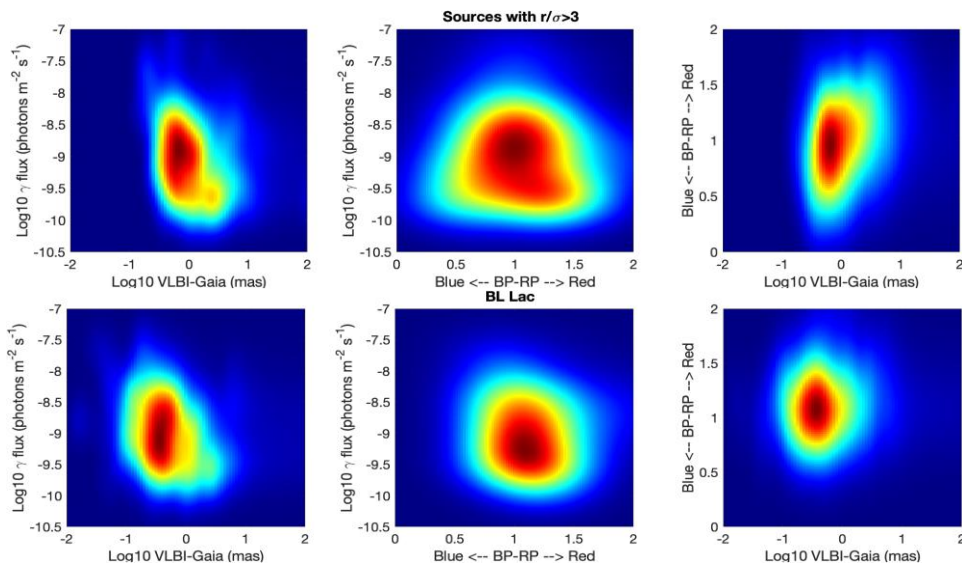


Fig.5 - KSD of the same distributions as in Fig.3 for the sub-sample of sources with large separation (upper panel, for $r/\sigma > 3$), and for the sub-sample of BL Lacs (lower panel).

The KSD approach offers additional insights by focusing on the sources with high r and on the BL Lacs (Fig.5). The patterns then appear more complex. High r sources are distributed into two subgroups, namely subgroup A (intermediate r , higher F_γ and intermediate color) and subgroup B (higher r , weaker F_γ , and the reddest color indices at the largest r). Both subgroups seem to follow the general trend of smaller F_γ for larger r . The significance of these two subgroups needs to be confirmed but they somewhat resemble subgroups 1 and 2 suggested by Fig.3 for BL Lacs. However the distribution of BL Lacs into two subgroups is less obvious in Fig.5. The KSD pattern appears more concentrated towards intermediate color indices ($BP-RP \geq 1$) for the BL Lacs than for high r sources. The peculiar KSD pattern in $F_\gamma - r$ for BL Lacs may still suggest two families of BL Lacs, one at smaller F_γ (and slightly smaller r) and a second one at higher F_γ (and slightly higher r). This highlights the complexity of the behavior of F_γ and requires further investigation.

3. Conclusion and perspectives

Detailed studies combining astrometric VLBI, *Gaia* and MOJAVE data on AGN showed that about 90% of *Gaia* centroids are coincident either with the VLBI radio core or with a radio knot in the VLBI jet. In the parameter space « $r - \text{gamma-ray flux } F_\gamma - \text{optical color index}$ », where r is the separation between the radio and the optical centroids, the "ICRF3/*Gaia*/LAT" sample of AGN shows strong similarities between the population of "low r sources" and "FSRQ", and between the population of "high r sources" and "BL Lacs".

For high separation sources, the *Gaia* centroid provides an interesting tool to locate the γ -ray emitting site with an accuracy of 0.1 mas. Two subgroups seem to appear at intermediate and higher separation, with decreasing activity (lower F_γ and redder color index) for increasing separation. Otherwise for low separation sources, the *Gaia* centroid can also accurately locate the dominant γ -ray site for BL Lacs but the situation is more difficult for FSRQ which require to disentangle the optical synchrotron emission from the disk contamination. Future better astrometric accuracies and spectral and polarimetric optical data should help in this regard.

Next steps will be to introduce redshifts, classification of BL Lacs (HBL, IBL, LBL), and other characteristics of the sources, to update the samples with new *Gaia* releases and improved VLBI catalogs, and to consider temporal evolution of astrometric and photometric quantities, taking into account proper motions when available. Improving reference frames will improve the modeling of AGN jets, while improving modeling of AGN jets will improve the reference frames.

References

- [1] Abdollahi, S., et al, Incremental *Fermi* Large Area Telescope Fourth Source Catalog (2022)
- [2] Brown, A.G.A., et al, A&A, 649, A1 ((2021)
- [3] Charlot, P., et al, A&A, 644, A159 (2020)
- [4] Kovalev, Y.Y., et al, MNRAS Lett, 493, L54 (2020)
- [5] Kramarenko, I., et al, MNRAS, 510, 469 (2022)
- [6] Lambert, S., et al, A&A, 651, A64 (2021)
- [7] Lico, R., et al, A&A, 658, L10 (2022)
- [8] Lister, M.L., et al, ApJ, 923, 30 (2021)
- [9] Mignard, F., et al, A&A, 595, A5 (2016)